Investigation into Speed and Temperature Field of Metal Drop in High-melting Metal Arc Spraying

S. Wang, C. H. Li* and Y. C. Ding

School of Mechanical Engineering, Qingdao Technological University, 266033 China
**Corresponding author E-mail: sy_lichanghe@163.com*

Abstract

This study was focused on the theoretical modeling and numerical simulation about the speed and temperature field of metal drop in high-melting metal arc spraying. The influences of the metal drop speed and temperature field in high-speed flight temperature distribution cloud chart and different air pressures on grain's flying speed were investigated. The result showed that, the highest speed of jet flow at the outlet of the spray gun reaches 600m/s; the air velocity quickly reduces to subsonic velocity after ejection within the spraying distance of 0-250mm . The air velocity continuously reduces along with the spraying distance increases. It is found that the grain's flying speed increases along with air pressure increase with the biggest speed within 200-250m/s and the grain's accelerated speed increases along with increase of air pressure and airflow speed when the spray gun structure is unchanged. Grain diameter has obvious influence on jet flow grain's flying speed.

Keywords: *High-melting metal arc spraying; Speed field; Temperature field; Metal drop; Flow field*

1. Introduction

The rapid moulding technology of metal arc spraying is a reproduction moulding technology thatwith physical model (or called prototype) as female die and arc as heat source, the melting metal materials are atomized with high speed airflow to form spraying grains, which are made to jet and deposit on the surface of female die to form compact metal coating in fixed thickness, known as die shell. Since the die shell accurately copies the prototypical shape and gets the necessary die cavity, the die's rapid manufacture is completed after reinforcement, demoulding, polishing and other post-processing technology. The process flow of metal arc spraying moulding is shown in Figure 1, mainly including: female die preparation; female die surface pretreatment; metal arc spraying; filling lining materials; demoulding and post-processing, etc. As a matter of fact, metal arc spraying rapid moulding technology is near net-shape rapid moulding technology.

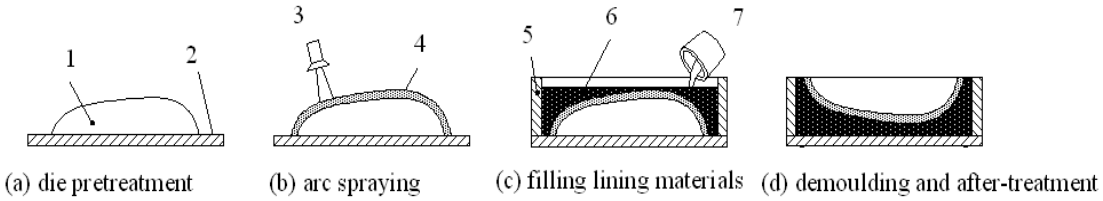

Figure 1. The Process Flow Chart of Metal Arc Spraying Moulding

The arc spraying mould making usually does not require for additional mechanical processing after accomplishment and , could be directly used for shaping manufacture. The numerical control finish machining for a little cutting output is required according to actual situation and demand to obtain higher shape precision, size precision and surface quality [1-8].

Metal arc spraying moulding technology takes female die as the standard that the die cavity size and geometric precision are completely from female die. Since cavity surface and its fine figure are formed at the same time, so it features in fast moulding speed, short moulding cycle, low cost and longer service life for the die. The processing cycle is 1/3-1/10 of the traditional steel die numerical control and the expense is 1/3-1/5 or lower [9-11], which becomes an important way for new product development and small lot production. Presently, this rapid moulding technology has been widely applied to airplane, automobile, appliance, furniture, shoemaking, art-ware and other industries. In various injected shaped dies with complicated surface shapes and fine figures, the characteristic details for figure duplication could be 5μm. The deformation in a whole is very small since the material's phase change partition is occurred in spraying complex and phase change transformation could be made up from the neighboring area, which is different from the casting process that its transformation is big for its overall phase change.

The middle and low melting metal arc spraying rapid moulding technology represented with zinc or zincaluminium alloy, etc has been applied in die development and sample automobile manufacture of large automobile panel, showing huge technological value and good economic benefit upon its fast and low cost features. However, since the hardness of zinc and zinc aluminium alloy is relatively low, the die's service life and application scope is restricted to certain extent. It is extremely attractive to manufacture arc spraying die with high melting point and high hardness metal (carbon steel and alloy steel) not only because the material is relatively cheap but also the die shell with high hardness and strength could greatly improves the service life of spraying die thus to expand the application scope of spraying die to provide better service for forming manufacture industry. However. the high melting point metal has bigger coating contractibility rate, thermal stress and porosity in spraying and the coating is easy for cracking, warping or spalling, making it diffidult to manufacture die shell and hard to control technological parameters [12-14]. Theoretical analysis and experimental research have been done for high melting point metal arc spraying technological parameters in this paper.

2. Analytical and Numerical Investigation of Flow Field

The grain deposition process is divided into two stages: in the first stage, the mutual effect of metal drop with airflow in flying process; the second stage, the metal drop collides with matrix to freeze and deposit. In the first stage, the metal drop produced by high pressure airflow atomization speeds up to fly towards matrix under high pressure and airflow effect and cool in the high pressure airflow. According to different metal drop and cooling speed, the metal particles are existed in complete liquid, semi-solid and solid states before striking the matrix. The proportions of metal particles in various states determine the average temperature of metal jet flow. Since the grain's flying time is only 1ms with fast flying speed and rapid temperature change together with the bad condition around jet flow, it is hard to directly detect jet flow state with experimental devices. The research method is mainly numerical calculation and simulation analysis. The change process between high speed flying grain speed and temperature in the jet

flow has been quantitatively analyzed with the combined method of FLUENT numerical simulation and experimental analysis.

2.1. Flow Field Modeling

Since the spray gun and its jet flow are axial symmetry structure, in order to simplify the calculation, the current conduction nozzle in the spray gun is ignored. The triangle gridding is adopted for division, the boundary conditions are: inlet pressure 0.5MPa, outlet pressure 0MPa and the initial pressures of up and down wall surfaces in jet flow area 0MPa.

The sprayer nozzle increases air velocity by changing section's geometric dimension in a short route. In the sprayer nozzle firstly contracted and then magnified, the subsonic velocity airflow speeds up in the reducing pipe; the sound velocity appears at the minimum section, which is accelerated to be supersonic speed after entering into increasing coupling. It is assumed that the air is the ideal gas, meaning gas's viscosity is not considered. The airflow is isentropic, zero friction and heat insulation that it flows in straight line from the inlet to the outlet. The gas has compressibility.

According to gas jet dynamics principle, the speed of compressed jet flow at the outlet could be calculated with the following formula [15]:

$$V_e = \sqrt{\frac{TR}{M} \cdot \frac{2k}{k-1} \cdot \left[1-\left(P_e/P\right)^{(k-1)/k}\right]} \quad (1)$$

In the formula:

V_e =exhaust velocity at outlet of sprayer nozzle, m/s;

T =thermodynamics temperature of the air at inlet, K;

R =common air constant, (8314.5 J/(kmol•K);

M =air molecule quality, kg/kmol;

k =cp/cv=adiabatic index;

cp=air specific heat at constant voltage;

cv=air specific heat at constant volume;

P_e =air absolute pressure at outlet, Pa;

P = air absolute pressure at inlet, Pa;

The Figures 2-3 are the velocity change of airflow axial along with axial distance. Seen Figure 6 and Figure 7 for simulation result, at the spray gun outlet, the highest air speed reaches 600m/s with violent disturbance wave. After ejection, the air velocity rapidly reduces to subsonic velocity (about 200m/s) within the spraying distance of 0-250mm. The air velocity continuously decreases along with greater of spraying distance. The high speed air atomizes metal molten drop, drives metal drop to accelerate flying towards the matrix and meanwhile quickly cools the high temperature molten drop.

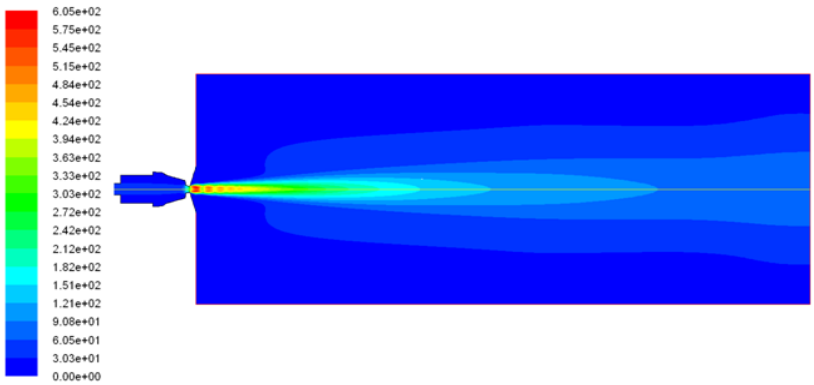

Figure 2. Velocity Field Nephogram of Melted Metal Airflow

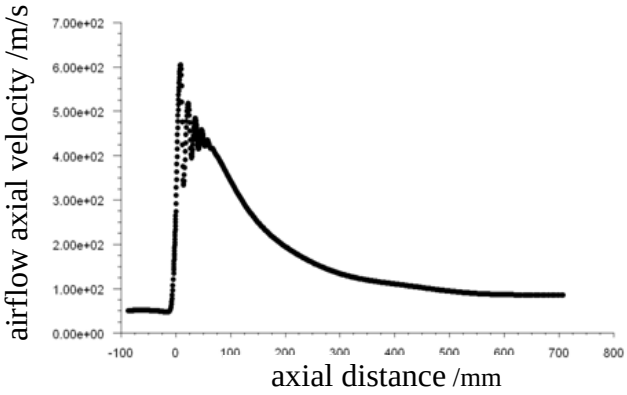

Figure 3. The Change of Airflow Axial Velocity Along with Axial Distance

2.2. Analysis of Numerical Results

Based on continuous phase analysis, load dispersed phase and conduct secondary calculation. Table 1 is dispersed phase parameter. The boundary conditions are: initial temperature 3000K, initial speed 0m/s, particle diameter 25μm and flow 0.00139kg/s. The loaded result of dispersed phase is shown in Figures 4-5.

Table 1. Dispersed Phase Parameters of 3Cr13 Material

Items	Values
melting point (℃)	1482
boiling point (℃)	300s
density (kg/m^3)	7.89e3
specific heat capacity (J/kg·K)	460
thermal conductivity (W/m·k)	24.9

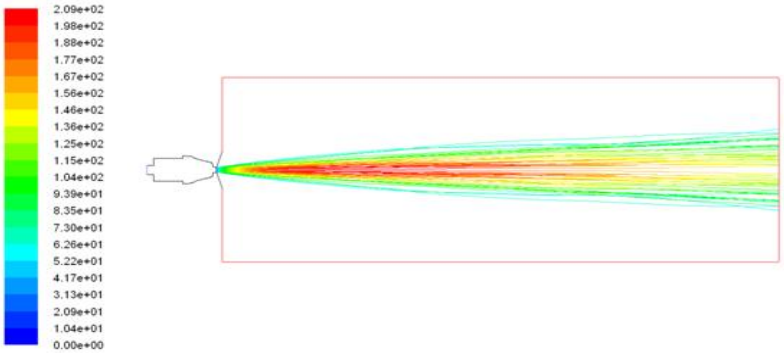

Figure 4. Velocity Distribution Nephogram of Melted Metal Airflow

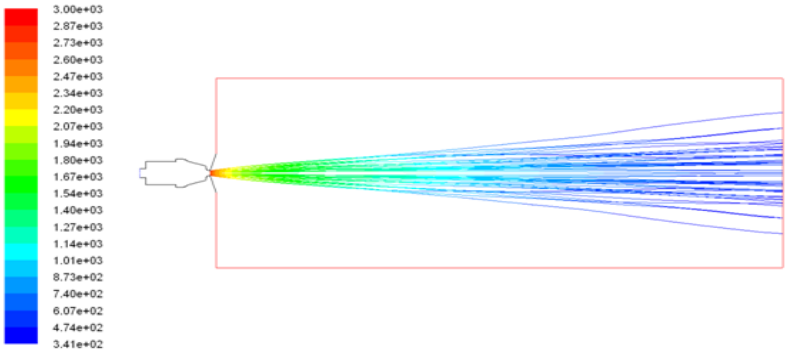

Figure 5. Temperature Distribution Nephogram of Melted Metal Airflow

According to aerodymanics principle, the change of gas axial velocity along with axial distance x is represented as [16]:

$$V_g = V_{gi} \exp\left(-\frac{x}{\lambda}\right) \tag{2}$$

In the formula, Vgi is air speed at the outlet and λ is the attenuation coefficient (0.1 ~ 0.3).

The total acting force F received by spherical metal drop with diameter of d is represented with the following formula:

$$F = m\left(dV_d/dt\right) = C_D\rho_g\left(V_g\text{-}V_d\right)^2 \cdot A/2 \tag{3}$$

A is sectional area of metal drop.

The accelerated speed of metal drop:

$$dV_d/dt = 3C_D\rho_g\left(V_g - V_d\right)\left|V_g - V_d\right|/4d\rho_d \tag{4}$$

The C:\Users\Program Files\Youdao\Dict\resultui\queryresult.htmldrag coefficient CD is related to Reynolds number[17].

$$C_D = 0.28 + \left[6/\mathrm{Re}\right]^{1/2} + \left[21/\mathrm{Re}\right] \tag{5}$$

The influence of different air pressures on grain's flying speed has been analyzed in the Fig.6 with 25μm- diameter grain as the research object that the grain's flying speed

increases along with air pressure increases with the maximum speed distributed in 200-250m/s. When the spray gun structure is unchanged, the airflow velocity increases along with air pressure increases and the grain's accelerated speed increases accordingly. The influence of air pressure on grain's speed has been gradually decreased when the pressure is over 0.5MPa. The speed almost has no change in 0.7~0.8MPa. The particle acceleration area is within 0.1 m of the spraying distance. When the spraying distance is between 0.1~0.3m, through fully accelerated, the spraying particle has high flying speed.

Seen from Figure 7, the grain diameter has obvious influence on flying speed of the jet flow particles. Under the precondition to ignore gravity, seen from the formula, the grain's accelerated speed will decrease along with grain diameter increases.

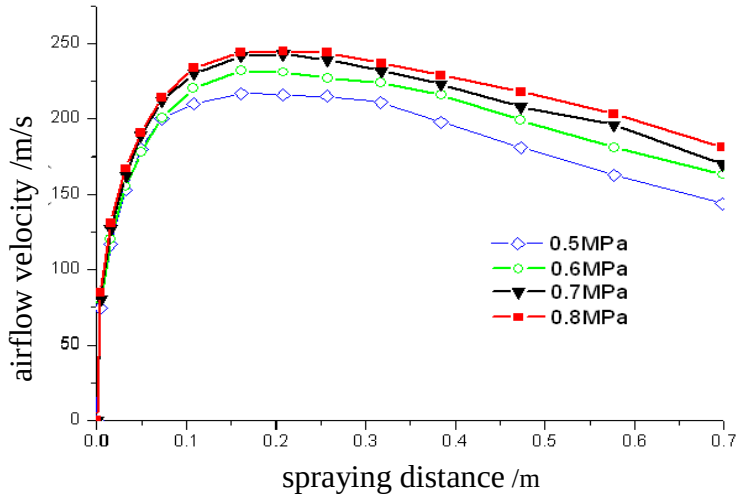

Figure 6. The Effect of Different Air Pressures on Airflow Velocity

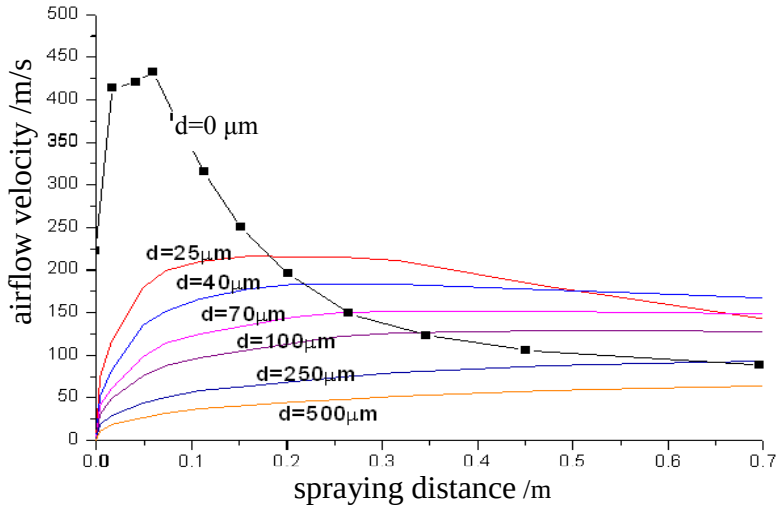

Figure 7. The Effect of Different Metal Grain Diameter on Airflow Velocity

For the given metal drop, its initial temperature Ti is determined by arc spray gun power and spraying velocity. The overheated liquid molten drop scatters its own heat to the surrounding air through convection and radiation. When liquid cooling is occurred, the molten drop with smaller size even has nucleation or solidification. The molten drop cooling satisfies Newton heat exchange condition. According to Ranz-Marshall relationship, the heat convection coefficient h is expressed as:

$$h = \frac{k_g}{d}\left(2 + 0.6\sqrt{R_e} \cdot \sqrt[3]{P_r}\right) \tag{6}$$

In the formula, kg is gas thermal conductivity, d is molten drop diameter and Pr is Prandal constant.

Since molten drop has high flying speed, the flying time is relatively short. Additionally, the molten drop has high superheat in arc spraying process, thus, most molten drops will not have solidification at atomization stage. The temperature distribution of molten drop with diameter of d in the atomization process is:

$$\frac{dT}{dt} = \frac{\Delta H_d}{C}\frac{df_s}{dt} - \frac{6h}{d\rho_d C}\left(T - T_g\right) \tag{7}$$

In the formula, T is molten drop temperature, t is flying time, Tg is gas temperature, C is the specific heat of molten drop(WhenT1 <T< T0, C= C1 is the specific heat of liquid phase; when Ts <T≤Tl, C= Cpd is the specific heat of solid and liquid mixture; when T≤Ts, C= Cs is the specific heat of solid phase), ΔHd is crystallization latent heat in unit mass, T_l is liquidus temperature, f_s is solid phase mark. In Schiel equation:

$$f_s = 1 - \left(\frac{T_m - T_l}{T_m - T}\right)^{\frac{1}{1-k_e}} \tag{8}$$

In the formula, T_m is the melting point of pure dissolvent (Fe) and k_e is balanced distribution coefficient of solute.

The temperature distribution of grains under different air pressures along with jet flow axis is shown in the Figure 8. In the flying stage, the grain's cooling speed continuously decreases along with grain's temperature decreases and the air velocity has little influence on grain's temperature. However, under the same air pressure spraying condition, grains in different diameters have obvious changes for the temperature, just as shown in the Figure 9. The melting point of stainless steel material 3Cr13 is 1482℃. When the grain temperature in small diameter is lower than the melting point temperature, since the flying speed is unable to reach cold spraying condition (500m/s), the grain is possible not to be deposited for rebounding.

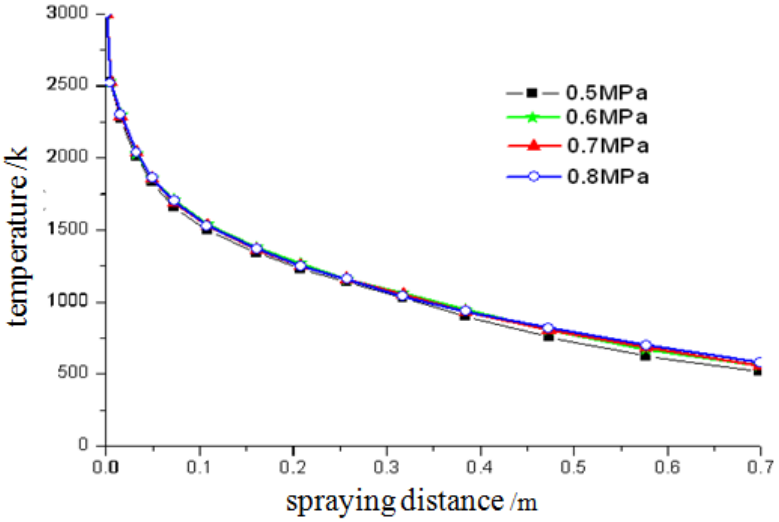

Figure 8. The Temperature Distribution of Grains under Different Pressures Along with Jet Flow Axis

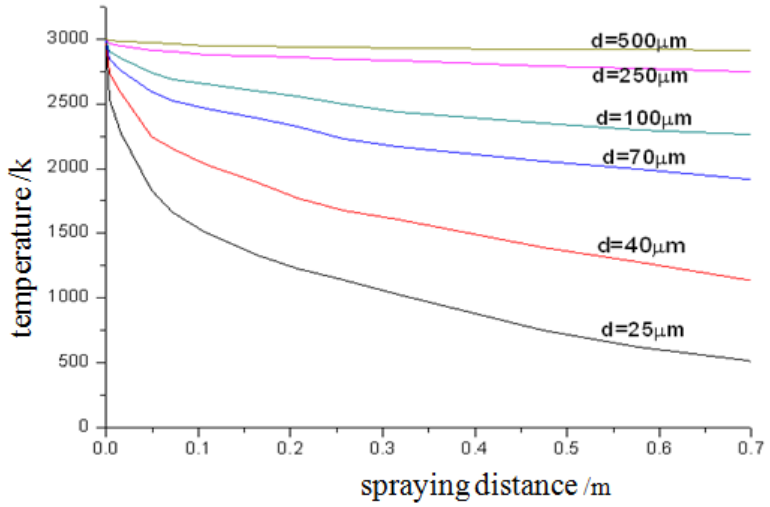

Figure 9. The Temperature Distribution of Grains under Different Diameter Along with Jet Flow Axis

3. The Experimental Results of Jet Flow

SprayWatch thermal spraying jet flow inspection device is adopted to detect grain's flying speed and temperature change in the jet flow.

SprayWatch is used to measure spraying grain's temperature, speed and flow, etc with CD camera with high speed shutter combined with digital imaging technology, spectrum resolving optics and other technologies. Seen in the Figure 10, SprayWatch monitor spraying jet flow is used to measure grain's speed and temperature in every 30mm along with jet flow axis within the scope of spraying distance of 90-270mm. The experimental result is shown in the Table 2.

Figure 10. SprayWatch Thermal Spraying Jet Flow Inspection Device

Table 2. The Experimental Results of Grain's Speed and Temperature

Spraying distance (mm)	90	120	150	180	210	240	270
Temperature (K)	2702	2716	2710	2786	2739	2723	2725
Velocity (m/s)	66.73	67.79	70.4	66.85	64.56	63.38	65.61

The jet flow grain speed is 60-70m/s and the jet flow grain temperature is 2700-2800K within the spraying distance scope of 100-300mm. What is unexpected: the grain speed and temperature have little change within the flying distance of 200mm. Seen from Figures 11 and 12, the error between simulation value and the experimental value of jet flow grain is only 5.5% and the error between simulation value and the experimental value of jet flow grain speed is only 14.1%. The matching of speed and temperature testifies the reliability for research result of grain's temperature and speed.

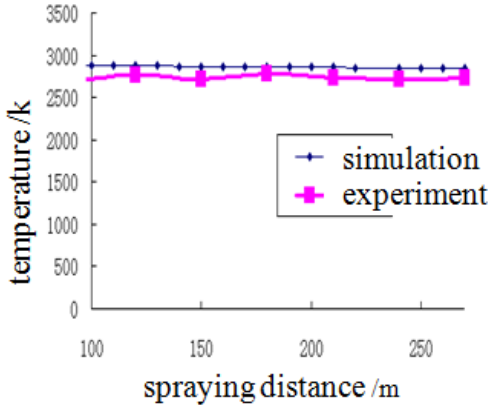

Figure 11. The Temperature Compares Simulation with Experimental Value

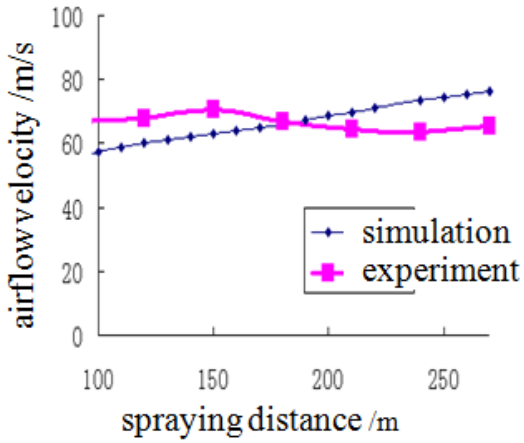

Figure 12. The Airflow Velocity Compares Simulation with Experimental Value

4.Conclusion

On the basis of the analysis results, the following conclusions are drawn:

(1)The combined method of numerical simulation and experimental analysis is used to quantitatively analyze for the change process of grain speed and temperature in high-speed flight in the jet flow and jet flow speed and temperature distribution cloud chart. The result showed that, the highest speed of jet flow at the outlet of the spray gun reaches 600m/s; the air velocity quickly reduces to subsonic velocity (about 200m/s) after ejection within the spraying distance of 0-250mm . The air velocity continuously reduces along with the spraying distance increases.

(2) The influence of different air pressures on grain's flying speed is analyzed with grain of 25μm diameter. It is found that the grain's flying speed increases along with air pressure increase with the biggest speed within 200-250m/s and the grain's accelerated speed increases along with increase of air pressure and airflow speed when the spray gun structure is unchanged. Grain diameter has obvious influence on jet flow grain's flying speed. Under the precondition to ignore gravity, the grain's accelerated speed decreases along with grain's diameter increase. In the flying stage, grain's cooling speed is also continuously decreasing along with grain's temperature decrease. The air velocity has little influence on grain's temperature. However, for the grains in different diameters under the same air pressure spraying condition, the temperatures have obvious changes.

Acknowledgements

This research was financially supported by the National Natural Science Foundation of China (50875138; 51175276); the Shandong Provincial Natural Science Foundation of China (ZR2009FZ007) ; Qingdao science and technology program of basic research projects（12-1-4-4-(1)-jch）and the Specialized Construct Fund for Taishan Scholars.

References

[1] J. -S. Chen, K. -W. Chen, "Bearing Load Analysis and Control of a Motorized High Speed Spindle", International Journal of Machine Tools & Manufacture, vol. 45, no. 12-13, **(2005)**, pp. 1487-1493.
[2] R. J. Gu, M. Shillor, G. C. Barber, et. al., "Thermal Analysis of the Grinding Process", Mathematical and Computer Modelling, vol. 39, no. 9-10, **(2004)**, pp. 991-1003.
[3] V. K. Gviniashvili, N. H. Woolley and W. B. Rowe, "Useful coolant flowrate in grinding", International Journal of Machine Tools & Manufacture, vol. 44, no. 6, **(2004)**, pp. 629-636.
[4] T. Jin and D. J. Stephenson, "Investigation of the heat partitioning in high efficiency deep grinding", International Journal of Machine Tools & Manufacture, vol. 43, no. 11, **(2003)**, pp. 1129–1134.
[5] T. Jin, W. B. Rowe and D. McCormack, "Temperatures in deep grinding of finite workpieces", International Journal of Machine Tools & Manufacture, vol. 42, no. 1, **(2002)**, pp. 53–59.
[6] T. Jin and G. Q. Cai, "Analytical thermal models of oblique moving heat source plane for deep grinding and cutting", ASME Journal of Manufacturing Science and Engineering, vol. 123, no. 2, **(2001)**, pp. 185-190.
[7] A. S. Lavine, "An exact solution for surface temperature in down Grinding", International Journal of Heat and Mass Transfer, vol. 43, no. 24, **(2000)**, pp. 4447-4456.
[8] D. S. Lee and D. H. Choi, "Reduced weight design of a flexible rotor with ball bearing stiffness characteristics varying with rotational speed and load", Journal of Vibration and Acoustics-transactions of the ASME, vol. 122, no. 3, **(2000)**, pp. 203-208.
[9] C. H. Li, Y. L. Hou, Y. C. Ding and G. Q. Cai, "Feasibility investigations on compound process: a novel fabrication method for finishing with grinding wheel as restraint", International Journal of Computational Materials Science and Surface Engineering, vol. 4, no. 1, **(2011a)**, pp. 55 – 68.
[10] C. H. Li, Y. L. Hou, Z. R. Liu and Y. C. Ding, "Investigation into temperature field of nano-zirconia ceramics precision grinding", International Journal of Abrasive Technology, vol. 4, no. 1, **(2011b)**, pp. 77 – 89.
[11] C. H. Li, Z. L. Han, C. Du and Y. C. Ding, "Numerical Study on Critical Speed Modeling of Ultra-high Speed Grinder Spindle", Communications in Computer and Information Science, vol. 201, **(2011c)**, pp. 202-209.
[12] C. H. Li, Y. L. Hou, C. Du and Y. C. Ding, "An Analysis of the Electric Spindle's Dynamic Characteristics of High Speed Grinder", Journal of Advanced Manufacturing Systems, vol. 10, no. 1, **(2011d)**, pp. 159–166.
[13] M. N. Morgan, A. R. Jackson and H. Wu, "Optimisation of fluid application in grinding", CIRP Annals-Manufacturing Technology, vol. 57, no. 1, **(2008)**, pp. 363-366.
[14] P. N. Moulik, H. T. Y. Yang and S. Chandrasekar, "Simulation of thermal stresses due to grinding", International Journal of Mechanical Sciences, vol. 43, no. 3, **(2001)**, pp. 831-851.
[15] D. J. Stephenson, T. Jin and J. Corbett, "High efficiency deep grinding of a low alloy steel with plated CBN wheels", Annals of the CIRP, vol. 51, no. 1, **(2002)**, pp. 241–244.
[16] S. C. Xiu, C. X. Chao and S. Y. Pei, "Experimental research on surface integrity with less or non fluid grinding process", Key Engineering Materials, vol. 487, **(2011)**, pp. 89-93.
[17] L. Zhu and W. Wang, "Modeling and Experiment of Dynamic Performance of the Linear Rolling Guide in Turn-milling Centre", Advanced Science Letter, vol. 4, no. 6, **(2011)**, pp. 1913–1917.

Authors

S. Wang is a graduate student at the School of Mechanical Engineering of Qingdao Technological University and has a interest in grinding and abrasive finishing, in particular CNC grinding; superabrasive grinding wheels; minimum quantity lubrication (MQL) grinding; simulation of grinding processes.

C. H. Li was awarded a PhD from the Northeastern University, China, in 2006. He is now a professor at the School of Mechanical Engineering of Qingdao Technological University. His research interests include computer applications in the study of surface finish mechanism; materials removal rate; abrasive finishing; quick-point grinding; surface roughness and integrity; CNC grinding; superabrasive grinding wheels; minimum quantity lubrication (MQL) grinding; grinding temperature field modeling; simulation of grinding processes; and high speed machining.

Y. C. Ding is now a Professor at the School of Mechanical Engineering of Xi'an Jiaotong University, and is the Taishan Scholar of Qingdao Technological University. He has a wide range of research experience and interest in advanced manufacturing technology, in particular high efficiency abrasive finishing; rapid tooling and micro-machining.